International Journal of Pharmaceutics 377 (2009) 159–168

Contents lists available at ScienceDirect

International Journal of Pharmaceutics

journal homepage: www.elsevier.com/locate/ijpharm

Pharmaceutical Nanotechnology

Anti-inflammatory and anti-oxidant activity of anionic dendrimer–N-acetyl cysteine conjugates in activated microglial cells

Bing Wang[a,c], Raghavendra S. Navath[b,c], Roberto Romero[c], Sujatha Kannan[a,**], Rangaramanujam Kannan[b,c,*]

[a] Department of Pediatrics (Critical Care Medicine), Children's Hospital of Michigan, Wayne State University, Detroit, MI 48201, USA
[b] Department of Chemical Engineering and Material Science, Wayne State University, Detroit, MI 48202, USA
[c] Perinatology Research Branch, Eunice Kennedy Shriver National Institute of Child Health and Human Development, NICHD, NIH, DHHS, Detroit, MI 48201, USA

ARTICLE INFO

Article history:
Received 27 February 2009
Received in revised form 29 April 2009
Accepted 29 April 2009
Available online 20 May 2009

Keywords:
Dendrimers
PAMAM
Drug delivery
Neuroinflammation
N-acetyl cysteine

ABSTRACT

Dendrimers are emerging as potential intracellular drug delivery vehicles. Understanding and improving the cellular efficacy of dendrimer–drug conjugates, can lead to significant *in vivo* benefits. This study explores efficacy of anionic polyamidoamine (PAMAM–COOH) dendrimer–N-acetyl cysteine (NAC) conjugates for applications in neuroinflammation. The anti-oxidative and anti-inflammatory effects of PAMAM–$(COOH)_{46}$–$(NAC)_{18}$ conjugate is evaluated on microglial cells *in vitro*. Cell entry and localization of PAMAM–$(COOH)_{62}$–$(FITC)_2$ conjugate in BV-2 microglial cells were assessed using flow cytometry and confocal microscopy. ELISA assays were used to evaluate markers of oxidative stress (ROS, NO) and inflammation (TNF-α) after stimulation of microglial cells with lipopolysaccharides (LPS), following treatment with increasing doses of free N-acetyl-L-cysteine (NAC) or PAMAM–$(COOH)_{46}$–$(NAC)_{18}$ conjugate containing an equivalent molar concentration of NAC. Flow cytometry and confocal microscopy demonstrated the PAMAM–$(COOH)_{62}$–$(FITC)_2$ conjugate entered BV-2 cells rapidly with significant increase in fluorescence within 15 min and localized mostly in the cytoplasm. PAMAM–$(COOH)_{46}$–$(NAC)_{18}$ conjugate was non-toxic, and significantly reduced ROS, NO and TNF-α release by activated microglial cells after 24 h and 72 h stimulation of LPS following 3 h pre-treatment when compared to the same concentration of free NAC ($P < 0.05$ or $P < 0.01$). Anionic PAMAM dendrimer–NAC conjugate was synthesized with a glutathione sensitive linker for intracellular release. The non-toxic conjugate is a more effective anti-oxidant and anti-inflammatory agent when compared to free NAC *in vitro*. The conjugate showed significant efficacy even at the lowest dose (0.5 mM NAC), where the activity was comparable or better than that of free drug at 8 mM (16× higher dosage). The improved efficacy of the conjugate, when combined with the intrinsic neuroinflammation-targeting ability of the PAMAM dendrimers, may provide new opportunities for *in vivo* applications.

1. Introduction

Perinatal brain damage is a major cause of disability and death in infants. A significant fraction of babies who suffer brain damage during and around birth develop cerebral palsy. There is increasing evidence suggesting that infection involving the uterus during pregnancy can lead to cerebral palsy in the baby (Makki et al., 2008; Romero et al., 1998, 2006, 2007a,b; Gomez et al., 2007). Recent studies demonstrate that the main mechanism of brain damage is due to the activation of microglial cells in the fetal brain that release inflammatory markers leading to the death of normal brain cells. These activated cells are not normally found in the brain. Infection or inflammation can activate microglial cells and cause them to migrate to the brain where they damage the normal brain cells. Therefore, developing intracellular drug delivery strategies to deliver drugs to activated microglial cells may help in decreasing the neuroinflammation and in the attenuation of the white matter injury. However, diagnosis and drug therapy during pregnancy is still a challenge. Recent work on a pregnant rabbit model has been able to successfully capture neuroinflammation-induced cerebral palsy, and its treatment using an anti-inflammatory drug, N-acetyl cysteine.

Developments in the rapidly expanding field of nanomedicine are offering a variety of nanoscale delivery vehicles such as liposomes, nanoparticles, and dendrimers (Lee et al., 2005; Cheng et al., 2008; Villalonga-Barber et al., 2008). Dendrimers are monodisperse, tree-like polymers with a large density of tailorable,

* Corresponding author at: Department of Chemical Engineering and Material Science, Wayne State University, Detroit, MI 48202, USA.
** Corresponding author.
E-mail addresses: skannan@med.wayne.edu (S. Kannan), rkannan@eng.wayne.edu (R. Kannan).

0378-5173/$ – see front matter © 2009 Elsevier B.V. All rights reserved.
doi:10.1016/j.ijpharm.2009.04.050

functional groups that have potential to deliver drugs in a targeted manner to the site of action (Wolinsky and Grinstaff, 2008). Their nanoscale branching architecture size (~5 nm) enables them to be transported into cells. When this is combined with appropriate targeting mechanism and intracellular drug release profiles, conjugates of dendrimers can be potentially potent for a variety of therapeutic applications. Anionic PAMAM dendrimers are being explored as drug delivery vehicles in this study (Wiwattanapatapee et al., 2004). In addition to being highly non-cytotoxic compared to the cationic dendrimers, anionic dendrimers have shown to be highly effective in transcellular transport and has been used for oral delivery applications. Previous studies in cancer cells have also shown that efficacy of anionic PAMAM dendrimer–methotrexate (MTX) conjugates were significantly better than cationic PAMAM dendrimer–MTX conjugates (Gurdag et al., 2005). This difference has been at least partially attributed to differences in lysosomal residence times and intracellular drug release from anionic and cationic dendrimer–drug conjugates. We have previously reported the synthesis, efficacy, and drug release from cationic PAMAM-generation-4 dendrimer–N-acetyl-L-cysteine conjugates, where the conjugate showed a significantly better efficacy than the free drug, perhaps due to superior intracellular transport of the drug by the dendrimer, and its subsequent rapid release from the glutathione sensitive disulfide linker (Navath et al., 2008). Anionic PAMAM dendrimers may be more effective *in vivo* platforms compared to cationic PAMAM dendrimers for drug delivery applications, because of their better cytotoxicity profiles, and reduced protein binding (Malik et al., 2000). The efficacy of the anionic dendrimer conjugates will be compared with those of the previous conjugates, where other drugs (e.g. methotrexate and methyl prednisolone) were investigated (Khandare et al., 2005; Kolhe et al., 2003, 2006; Kannan et al., 2004).

N-acetyl-L-cysteine (NAC) is an anti-inflammatory and antioxidant agent used in a wide range of clinical applications (Wang et al., 2007). It is being explored for use in neuroinflammation in perinatal applications (Paintlia et al., 2008). NAC could effectively block CD11b expression in mouse BV-2 cells and primary microglia, which is correlated to the severity of microglial activation in various neuroinflammatory diseases reported (Roy et al., 2008). However, early pharmacokinetic studies suggested that oral NAC bioavailability was low, between 6% and 10%, due to low blood concentration of NAC. The biological half-life of NAC is only 1.5 h in the blood stream. Building on the recent findings that suggest that PAMAM dendrimers can target neuroinflammation, even after intravenous administration, this study seek build conjugates by understanding the efficacy in target cells (Kannan et al., 2007). Specifically, we investigate the anti-inflammatory and anti-oxidative effects of PAMAM dendrimer–NAC conjugate, compared to free NAC, on activated microglial cells, which are the target cells for this drug *in vivo*. The unique aspect of this study arises from the fact that the activity of the conjugated drug is being explored using *multiple assays*, for dendrimer–drug conjugates in non-cancer applications.

2. Materials and methods

2.1. Materials

Polyamidoamine (PAMAM) dendrimer (generation 3.5 with –COOH end groups) was purchased from Dendritech, USA. Other reagents were obtained from assorted vendors in the highest quality available. These include benzotriazol-1-yl-oxytripyrrolidinophosphonium hexafluorophosphate (PyBop, Aldrich), diisopropyl ethylamine (Aldrich) dimethyl sulfoxide (DMSO, Aldrich), dimethyl formamide (DMF, Aldrich), N-acetyl cysteine (NAC, Aldrich), glutathione (GSH, Aldrich), acetonitrile (Aldrich) phosphate buffer saline (PBS, pH 7.4, Aldrich), and Spectra/Por dialysis membrane (MWCO 1000). Dulbecco's Modified Eagle Medium, fetal bovine serum, penicillin–streptomycin, and 0.05% trypsin–EDTA were purchased from Invitrogen. 3-(4,5-dimethylthiazol-2-yl)-2,5-diphenyltetrazolium bromide and lipopolysaccharide (LPS) were purchased from Sigma. The Amplex Red hydrogen peroxide/peroxidase assay kit, nitrate/nitrite calorimetric assay kit, and mouse TNF-α ELISA Kit were purchased from Invitrogen, Cayman Chemical, and BD Biosciences, respectively.

2.2. Methods

All ^{1}H and ^{13}C NMR spectra were recorded on 400 MHz Varian Mercury spectrometer in DMSO. MALDI-TOF spectra were obtained using a Bruker Ultraflex system equipped with a pulsed nitrogen laser (337 nm), operating in the positive ion reflector mode, using 19 kV acceleration voltage and a matrix of 2,5 dihydroxybenzoic acid.

2.2.1. HPLC conditions

HPLC characterization of conjugates was carried out with Waters HPLC instrument equipped with two pumps, an autosampler and dual UV detector interfaced to Breeze software. The mobile phase used was acetonitrile–water (both 0.14% TFA by weight), and water phase had a pH of 2.25. Mobile phases were freshly prepared, filtered and degassed prior to the use. Supelco wide-pore C5 HPLC Column (5 μm particle size, 25 cm × 4.6 mm length × I.D.) equipped with two C5 Supelguard Cartridges (5 μm particle size, 2 cm × 4.0 mm length × I.D.) was used for characterizing the elution times and the stability of the conjugates and the reaction mixtures. Gradient method used for analysis was (100:0) Water: Acetonitrile to (60:40) Water–Acetonitrile in 25 min followed by returning to initial conditions in 5 min. The flow rate was 1 mL/min. The dual UV absorbance detector was used at 210 nm and 280 nm simultaneously. Calibration curves were prepared for NAC, GSH and their oxidized forms, based on UV absorbance peak area at 210 nm. These calibrations were used in the characterization and stability analysis.

2.2.2. Synthesis of PAMAM–$(COOH)_{46}$–$(NAC)_{18}$ conjugate

PAMAM–$(COOH)_{46}$–$(NAC)_{18}$ was prepared in three steps. The detailed synthesis and characterization of this conjugate is described elsewhere (Navath et al., 2008). A brief summary is offered here. In the first step, S-(2-thiopyridyl) glutathione was prepared from the reaction of 2,2[1]-dithiodipyridine in excess and the corresponding peptide in a mixture of methanol and water at room temperature. Upon completion of the reaction, methanol was removed *in vacuo* and the residue was washed with dichloromethane. The aqueous solution was subjected to reverse phase (RP)-HPLC purification, and lyophilization of the eluent gave the pure product as a white solid. In the second step, the above compound was reacted with NAC (1 eq) in PBS in pH 7.4 to get desired GS-NAC intermediate and purified. In third step, to introduce the GS-NAC, PAMAM–COOH was reacted with GS-NAC (64 eq/dendrimer) in the presence of PyBop/DIEA to give desired PAMAM–$(COOH)_{46}$–$(NAC)_{18}$ conjugate. Introduction of 18 GS-NAC was confirmed using HPLC, ^{1}H NMR (Fig. 1) and MALDI. The MALDI analysis of the PAMAM–$(COOH)_{46}$–$(NAC)_{18}$ conjugate suggested a molecular weight of 19.7 kDa (Fig. 2) (18 GS-S-NAC molecules on one PAMAM–COOH dendrimer, Table 2). The attachment of GS-S-NAC groups to the dendrimer was also confirmed using ^{1}H NMR analysis, as evidenced by the appearance of methyl protons at 1.70, 1.92 ppm that indicate the formation of GS-S-NAC conjugate with dendrimer.

2.2.3. Preparation of PAMAM–$(COOH)_{62}$–$(FITC)_2$ conjugate

The PAMAM G3.5–COOH dendrimer was tagged with fluorescent dye FITC in three steps. First, PAMAM–CO–NH–ethylene–NH–BOC

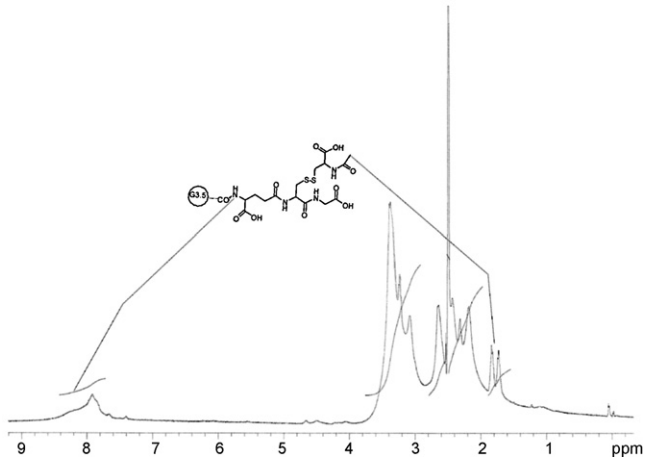

Fig. 1. ^{1}H NMR spectrum of the PAMAM-$(COOH)_{46}$-$(NAC)_{18}$ conjugate. The appearance of methyl protons at 1.70, 1.92 ppm indicating the formation of GS-NAC conjugate with dendrimer.

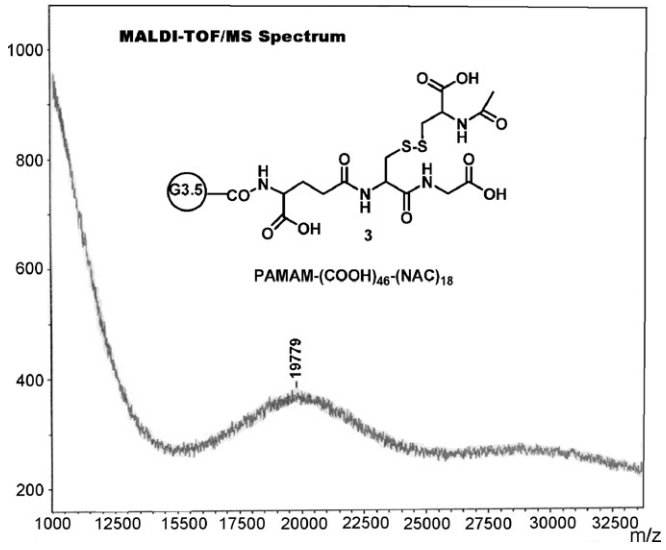

Fig. 2. MALDI-TOF spectrum of the PAMAM-$(COOH)_{46}$-$(NAC)_{18}$ conjugate.

was prepared by reacting appropriate amounts of PAMAM–COOH with BOC-protected ethylenediamine in the presence of PyBop and DIEA (500 μL) in DMSO/DMF (2:3, 2 mL). The reaction mixture was stirred at room temperature for 12 h. PAMAM–CO–ethylenediamine–BOC was purified using a dialysis membrane (MWCO 1000), first in DMSO, followed by PBS (pH 7.4), to remove by-products and the excess of reactants. The compound purified by further dialysis in deionized water (3 times) for 12 h to remove salts. After dialysis, the solvent was removed using a lyophilizer, resulting in the purified product. The MALDI analysis of this compound yielded a molecular weight of 13.7 kDa (Fig. 3), suggesting 37 NH–ethyl–NH–BOC groups per one molecule of the dendrimer. In the second step, PAMAM–CO–NH–ethylene–NHBOC was treated with trifloroacetic acid and dichloromethane (1:1). The reaction was stirred at room temperature for 2 h. After completion of the reaction trifloroacetic acid/dichloromethane was removed under rotavaporation. The reaction contents were neutralized (aq Na_2CO_3) (pH 7.4) and lyophilized to get the desired intermediate. In the third step, PAMAM–CO–ethylenediamine was labeled with FITC. In brief, two equivalent of FITC was dissolved in DMSO. DMSO solution of PAMAM–CO–NH–ethylene–NH_2 was added to FITC and the reaction was stirred at room temperature for 12 h in dark. The FITC-labeled compound was purified using a sephadex LH-20 column (Amersham Pharmacia Biotech, 3.8 × 45 cm) with water as mobile phase. Water was removed under lyophilization to get the pure FITC-labeled compound.

2.2.4. Cell culture

Mouse microglial cell line (BV-2) was obtained from Children's Hospital of Michigan Cell Culture Facility. Cells were grown in 75 mm^2 culture flasks using Dulbecco's Modified Eagle Medium (DMEM) supplemented with 5% fetal bovine serum (FBS) and 1% penicillin–streptomycin at 37 °C with 5% CO_2 in an incubator. The cells were subcultured every 48 h and harvested from subconfluent cultures (60–70%) using 0.05% trypsin–EDTA.

2.2.5. Flow cytometry analysis

BV-2 cells (passage 16) were grown overnight in a 6-well plate using DMEM cell culture medium supplemented with 5% FBS and 1% penicillin–streptomycin. When the cells were 70% confluent, they were treated with 10 μg/mL of FITC-labeled dendrimer (PAMAM–$(COOH)_{62}$–$(FITC)_2$) for 15 min, 60, 120 and 240 min. The

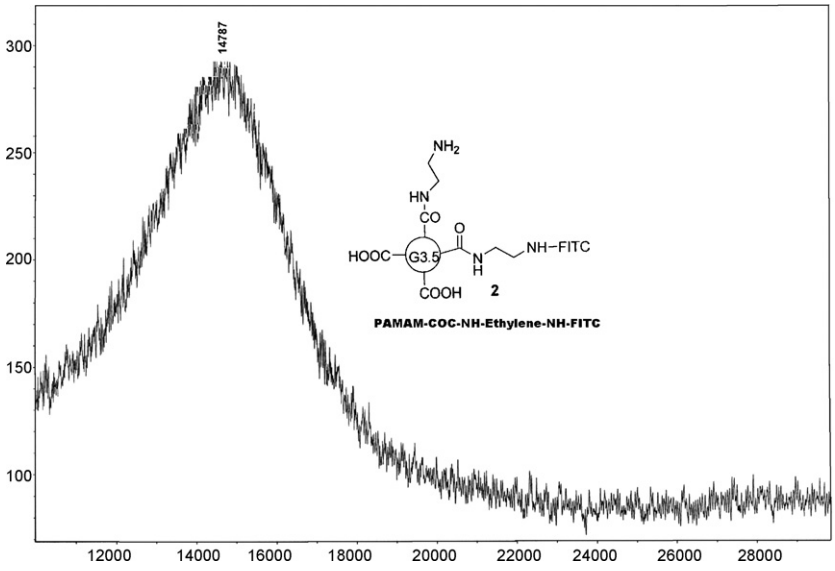

Fig. 3. MALDI-TOF spectrum of the PAMAM-$(COOH)_{62}$-$(FITC)_2$, that was used for flow cytometry and imaging experiments.

cells were washed with phosphate buffered saline (PBS, pH 7.4), trypsinized and centrifuged at 1500 rpm for 5 min to obtain a cell pellet. The cells were washed 3 times with PBS, and resuspended in 1% formaldehyde, and analyzed using a flow cytometer (FACS caliber, Becton Dickinson) by counting 20,000 events. The mean fluorescence intensity of cells was calculated using the histogram plot.

2.2.6. Confocal laser scanning microscopy

After treating BV-2 cells for 2 h with 10 μg/mL of PAMAM–$(COOH)_{62}$–$(FITC)_2$, the cells were washed with PBS 3 times and fixed with 4% para-formaldehyde for 20 min. Images were captured using a confocal microscope (Zeiss LSM 310) using a magnification of 400×. For FITC, the excitation and emission wavelengths were 488 nm and 518 nm respectively.

2.2.7. Cell cytotoxicity assay

Cell cytotoxicity was assessed by MTT assay. BV-2 cells (passage 16) were seeded into 96-well plate at 5×10^3/well, and incubated overnight at 37 °C. Two groups of experiments were performed, to test the effect of duration of dendrimer-drug treatment. In the first group, the cells were treated continuously for 24 h. To do this, the medium was removed, and the cells were exposed to 100 ng/mL of LPS and varying concentrations of PAMAM–$(COOH)_{46}$–$(NAC)_{18}$ conjugates in serum free medium for 24 h. In the second group, the cells were pre-incubated with 100 ng/mL of LPS and varying concentrations of PAMAM–$(COOH)_{46}$–$(NAC)_{18}$ conjugates for 3 h. After this, the cells were exposed to 100 ng/mL of LPS for 24 h. Control treatment with varying concentrations of free NAC or corresponding dendrimer, positive control (with 100 ng/mL of LPS induction), and negative control (with medium alone) were also utilized. In order to assess the cytotoxicity, 10 μL of MTT (5 mg/mL) was added to each well. After 4 h of incubation at 37 °C, the supernatant was removed, and 100 μL of DMSO was added to dissolve precipitated formazan crystals. The plate was shaken for 10 min. OD value was measured using a microplate reader at a wavelength of 570 nm. The proportion of viable cells in the treated group was compared to that of the negative control.

2.2.8. Cells treatment with PAMAM–$(COOH)_{46}$–$(NAC)_{18}$ conjugate

BV-2 cells (passage 16) were seeded in 24 well plates at 10^5/mL/well and incubated for 24 h. The medium was removed, and the cells were exposed to 100 ng/mL of LPS and varying concentrations of PAMAM–$(COOH)_{46}$–$(NAC)_{18}$ conjugate in 500 μL of serum free medium for 3 h. The medium was removed again, and 500 μL of fresh serum free medium containing 100 ng/mL of LPS was added and incubated for 24 h and 72 h. Control treatment with varying concentrations of free NAC, positive control with 100 ng/mL of LPS induction, but negative control without any LPS induction and treatment were also studied. The culture medium was collected at specific time intervals of 24 h and 72 h, and spun at 1500 rpm for 5 min. The supernatant was stored at −80 °C for further assays.

2.2.9. Measurement of ROS

H_2O_2 released from BV-2 cells was measured using 10-acetyl-3,7-dihydroxyphenoxazine (Amplex Red), following the manufacturer's instructions (Alexandre et al., 2006; Min et al., 2003). The procedure for cell culture and drug treatment was the same as described in previous section. The supernatant was mixed with 0.05 U/mL of horseradish peroxidase and 1 μM of Amplex Red in 96-well plates. After 30 min incubation, the fluorescence intensity was measured using spectrofluorometry. Excitation and emission wavelengths were 530 nm and 590 nm respectively.

2.2.10. NO release assay

Production of NO was assayed by measuring the levels of nitrite, the stable NO metabolite, in the culture medium. Accumulation of nitrite in the medium was determined by colorimetric assay with Griess reagent system, which uses sulfanilamide and N-(1-Naphthyl)-ethylene diamine. From the treated cells in the medium, 100 μL of the supernatant was incubated with 50 μL of Griess reagent 1 (sulfanilamide) and 50 μL of Griess reagent 2 N-(1-Naphthyl)-ethylenediamine for 10 min at room temperature. The absorbance at 540 nm was then measured, and nitrite concentration was determined using a calibration curve prepared using nitrite standards.

2.2.11. Detection of TNF-α

The procedure for cell culture and drug treatment was the same as described in previous section. TNF-α secretion was measured using an ELISA kit according to the manufacturer's instructions. In brief, 50 μL of supernatant from each sample was added in 96-well ELISA plates. Biotinylated antibody reagent was applied to each well and the plate was incubated at room temperature for 2 h. After washing the plate with PBS-Tween 20, diluted streptavidin-HRP was added, and the plate was incubated at room temperature for 30 min. After washing the plate, the premixed TMB substrate solution was added. The plate was developed in the dark for 30 min, and read at 450 nm using a microplate reader. The concentration of TNF-α was calculated using murine rTNF-α as standard.

2.2.12. Statistical analysis

Data are presented as mean ± SD. Specific comparisons between control and individual experiment were analyzed by Student's *t*-test with *P*-value less than 0.05 considered as statistical significance.

3. Results

3.1. Preparation and characterization of dendrimer–NAC conjugates

A PAMAM dendrimer conjugate [PAMAM–$(COOH)_{46}$–$(NAC)_{18}$] has been developed, using a disulfide linker, for glutathione (GSH)-mediated intracellular release of NAC. To facilitate the linking of NAC to dendrimer via disulfide bond spacer group, glutathione (GSH) were used. To prepare GS-NAC, GSH was reacted with 2,2[1]-dithiodipyridine to give GS-TP, which was further reacted with NAC to give GS-NAC. To introduce the GS-NAC, PAMAM–COOH was reacted with GS-NAC in the presence of PyBop/DIEA to give the desired PAMAM–$(COOH)_{46}$–$(NAC)_{18}$ conjugate (Fig. 2).

3.1.1. PAMAM–$(COOH)_{46}$–$(NAC)_{18}$ Conjugate

PAMAM–$(COOH)_{46}$–$(NAC)_{18}$ conjugates having cleavable disulfide linkages are designed for intracellular delivery based on glutathione levels. PAMAM–$(COOH)_{46}$–$(NAC)_{18}$ conjugate was synthesized using a three-step sequence. S-(2-thiopyridyl) glutathione was prepared from the reaction of 2,2[1]-dithiodipyridine and GSH, and purified through HPLC. This compound was reacted with NAC in PBS (pH 7.4) to get the desired Glutathione-N-Acetyl Cysteine (GS-S-NAC) intermediate upon purification. The formation of disulfide bond was confirmed by ^{1}H NMR and ESI-MS. Appearance of methyl groups in ^{1}H NMR at 1.90 ppm indicates the formation of disulfide bond between the GSH and NAC. To introduce the GS-S-NAC, PAMAM–COOH was reacted with GS-S-NAC in the presence of PyBop/DIEA to obtain the desired PAMAM––$(COOH)_{46}$–$(NAC)_{18}$ conjugate (Fig. 1). Introduction of GS-S-NAC was confirmed HPLC, ^{1}H NMR and MALDI. MALDI analysis yielded a molecular weight of 19.7 kDa (Fig. 2) (18 GS-S-NAC molecules for one molecule of PAMAM–COOH dendrimer). The number of GS-S-NAC groups was

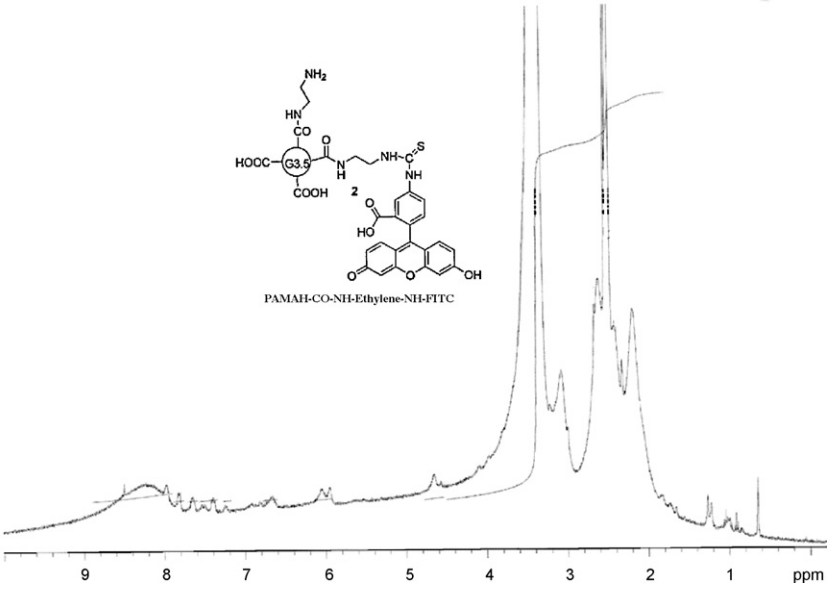

Fig. 4. ^{1}H NMR spectrum of the PAMAM-$(COOH)_{62}$-$(FITC)_2$ conjugate that was used for flow cytometry and imaging experiments.

also determined using ^{1}H NMR analysis (Fig. 1), with the appearance of methyl protons at 1.70, 1.92 ppm indicating the formation of GS-NAC conjugate with dendrimer. The ^{1}H NMR and the MALDI data for the drug payload agree very well with each other, as summarized in Table 1.

3.1.2. PA MAM–$(COOH)_{62}$–$(FITC)_2$ conjugate

PAMAM–COOH dendrimer was tagged with fluorescent dye FITC in three steps. PAMAM–CO–ethylene diamine–BOC was prepared by reacting PAMAM–COOH with BOC-protected ethylene diamine in the presence of PyBop/DIEA/DMSO/DMF. To couple FITC, tert-butyl group was deprotected with trifloroacetic acid and dichloromethane to get the desired partial amine functionality on dendrimers. The number of ethylene diamine molecules attached on the dendrimers was determined with MALDI and summarized in Table 1. PAMAM–CO–ethylene–NH_2 was labeled with FITC. DMSO solution of PAMAM–CO–ethylene–NH_2 was added to FITC and the reaction was stirred at room temperature in dark, and further purified using dialysis. The number of FITC groups was determined using MALDI and ^{1}H NMR. In the ^{1}H NMR spectrum, the appearance of aromatic protons at δ (ppm), 5.95–6.0(m, 1H), 6.05–6.12(m, 1H), 6.60–6.72(m, 1H), 7.20–7.30(d, J = 4 Hz, 1H), 7.38–7.42(m, 1H), 7.52–7.60(d, J = 4 Hz, 1H), 7.62–7.71(m, 1H), 7.80–7.90 (m, 1H) indicates the formation of FITC-conjugate with dendrimer (Fig. 4). The ^{1}H NMR and the MALDI data for the FITC payload agree very well with each other, as summarized in Table 1.

3.1.3. Release of NAC from PAMAM–$(COOH)_{46}$–$(NAC)_{18}$ conjugate

N-acetyl cysteine release from PAMAM–$(COOH)_{46}$–$(NAC)_{18}$ conjugate was analyzed at intracellular GSH concentration (10 mM). The detailed mechanism and kinetics of the drug release have been described elsewhere (Kurtoglu et al., 2009). Briefly, the results suggest that the conjugate was able to release significant amounts of free NAC within an hour, in the presence of GSH. In the absence of GSH, or at GSH levels in the blood (20 μM), no drug release was seen. PAMAM–$(COOH)_{46}$–$(NAC)_{18}$ conjugate released 39% of NAC in the free form and another 6% in the GS-S-NAC form within 1 h, yielding a total of 45% NAC release. Our eventual application, where neuroinflammation in the newborn rabbit pups is treated with the conjugates, requires relatively fast release of NAC from the conjugates. The release is desired over a period of a few days. The timescales for the cellular efficacy has been chosen to be 24 h or 72 h, with this *in vivo* requirement in mind.

3.2. Cell entry of PAMAM–$(COOH)_{62}$–$(FITC)_2$ conjugate in BV-2 microglial cells

Cellular entry of PAMAM–$(COOH)_{62}$–$(FITC)_2$ conjugate was evaluated using flow cytometry and confocal microscopy. The flow cytometry shows a significant fluorescence intensity increase within 15 min, as evidenced by a two-order of magnitude increase in the fluorescene intensity. There was a moderate increase in fluorescence over the next 4 h (Fig. 5). This showed that the PAMAM–$(COOH)_{62}$–$(FITC)_2$ conjugate entered the cells rapidly. The cellular entry was also visualized by using confocal microscopy. It is evident that the conjugate entered the cells and localized mostly in the cytoplasm, while the nucleus appears to be relatively free of the presence of fluorescence at 2 h. The cells without any treatment show no fluorescence (Fig. 6). The relatively rapid and appreciable uptake of the anionic dendrimer in these cells is significant, as anionic molecules are expected to have relatively weak interactions with the somewhat anionic cell membranes which may reduce uptake (Kim and Wogan, 2006; Lessio et al., 2005; Waseem et al., 2008). In fact, the anionic dendrimer conjugate

Table 1
Molecular weight estimation (by MALDI-TOF, and ESI-MS) of NAC, FITC in PAMAM–$(COOH)_{46}$–$(NAC)_{18}$, PAMAM–$(COOH)_{62}$–$(FITC)_2$ respectively.

Name of the compound	Molecular weight	Pay load	Purity of conjugate	Solubility in PBS/H_2O
GS-S-NAC	468 kDa	–	99.1%	Soluble
PAMAM–$(COOH)_{46}$–$(NAC)_{18}$	19.7 kDa	18	99.5%	Highly Soluble
FITC	389 Da	–	99.5%	Not Soluble
PAMAM–CO–NH–$(CH_2)_2$–NH_2	13.7 kDa	37	99.5%	Highly Soluble
PAMAM–$(COOH)_{62}$–$(FITC)_2$	~14.7 kDa	2	99.5%	Highly Soluble

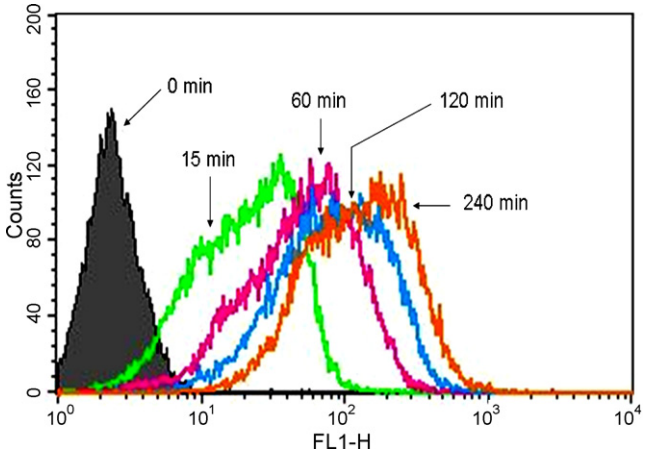

Fig. 5. Flow cytometry of the cell entry dynamics of PAMAM–$(COOH)_{62}$–$(FITC)_2$ conjugate in BV-2 microglial cell line. The log of FITC absorption intensity (FL1-H on *x*-axis) is plotted against the number of cells (counts on *y*-axis). The rapid increase cellular uptake of PAMAM–$(COOH)_{62}$–$(FITC)_2$ within 15 min is evident. The transport of conjugate into cells increased with increasing time.

enters these cells well. When this is combined with the better lysosomal localization of anionic dendrimers, better intracellular drug release from the conjugates may be observed (Perumal et al., 2008).

3.3. Cytotoxicity of cells treated with PAMAM–$(COOH)_{46}$–$(NAC)_{18}$ conjugate

The conjugate contained 18 NAC molecules per PAMAM–COOH dendrimer. So the dendrimer concentration in the conjugate, corresponding to a NAC concentration range of 0.5–8 mM, was 0.03–0.44 mM. The corresponding concentrations of free PAMAM–COOH dendrimer (0.03–0.44 mM) were also not toxic to the microglial cells. The free NAC did not show any toxicity at 0.5–8 mM to BV-2 cells (Fig. 7). MTT assay showed that PAMAM–$(COOH)_{46}$–$(NAC)_{18}$ conjugate was non-cytotoxic at 0.04–0.59 mM (the conjugate concentrations based on a drug concentration of 0.5–8 mM) after 24 h treatment and 24 h stimulation with 100 ng/mL of LPS following 3 h treatment. This suggests that all the compounds on which the efficacies were tested were non-cytotoxic, and that the efficacies differences were likely not due to cytotoxicity.

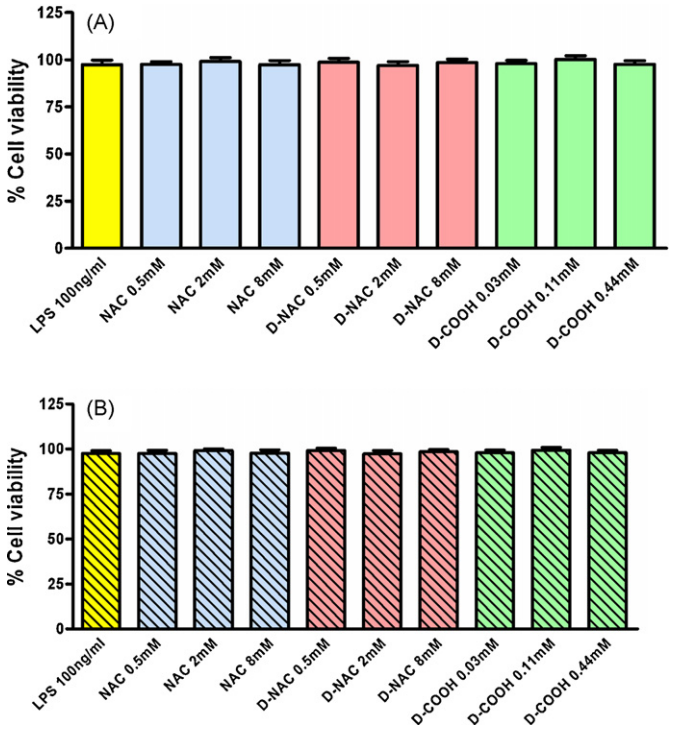

Fig. 7. Cytotoxicity assay. (A) BV-2 cells (passage 16) were co-treated with 100 ng/mL of LPS and the indicated concentration of NAC, PAMAM–$(COOH)_{46}$–$(NAC)_{18}$ conjugate and the corresponding amount of free dendrimer for 24 h. (B) Cells were stimulated with 100 ng/mL of LPS for 24 h following 3 h pre-treatment with NAC, PAMAM–$(COOH)_{46}$–$(NAC)_{18}$ conjugate and the corresponding amount of free dendrimer. Three samples were used for each group. Cell viability was assessed by MTT method. The proportion of viable cells in the treated group was compared to that of negative control.

3.4. Anti-oxidative activity of PAMAM–$(COOH)_{46}$–$(NAC)_{18}$ conjugate

The anti-oxidative properties of the conjugate were tested by measuring the reactive oxygen species (ROS) and free radical NO in activated microglial cells. This is an indication of the ability of the conjugates to treat neuroinflammation, since these cells play a central role in the disease process. In prior studies in activated cells, it has been observed that ROS and NO production at 72 h after activation was significantly higher than

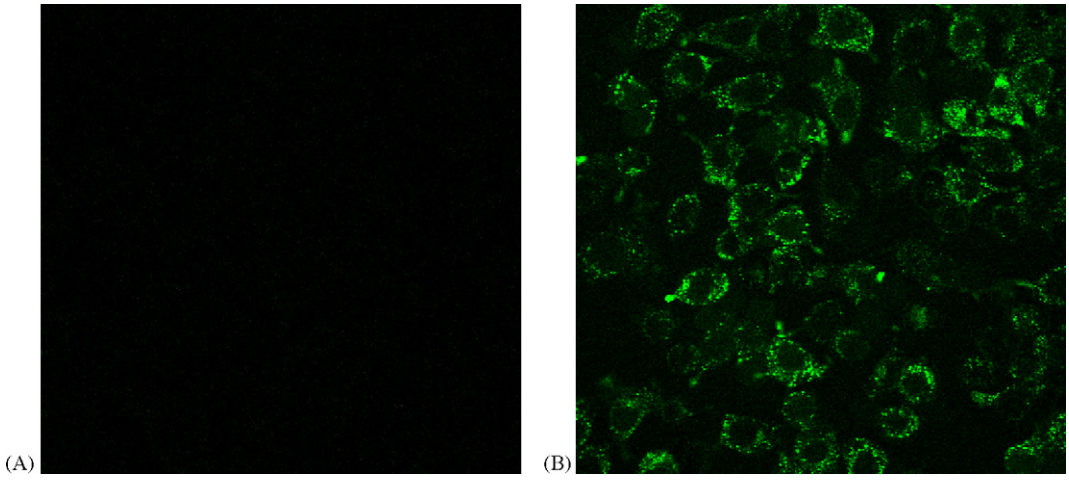

Fig. 6. Confocal microscopy images (400×) after 2 h of treatment with (A) control and (B) PAMAM–$(COOH)_{62}$–$(FITC)_2$. The PAMAM–$(COOH)_{62}$–$(FITC)_2$ conjugates appear to be mainly localized in the cytoplasm at this time point.

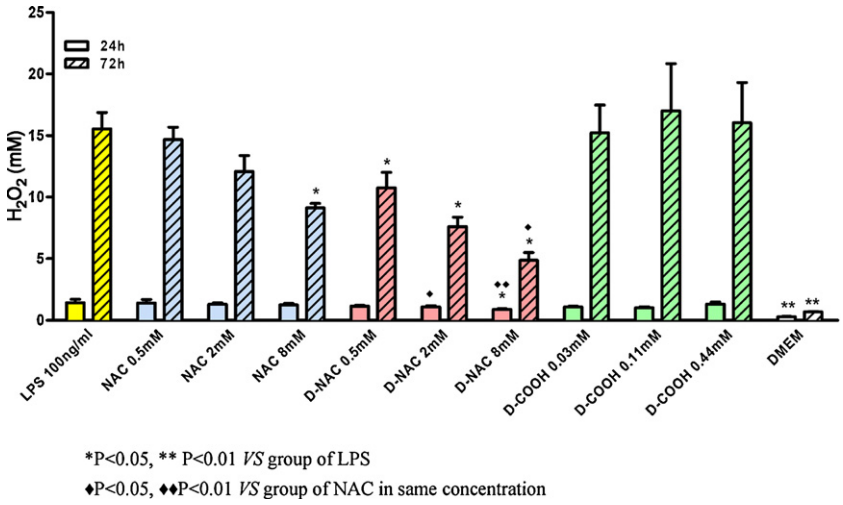

Fig. 8. ROS assay. BV-2 cells (passage 16) were stimulated with 100 ng/mL of LPS for 24 h and 72 h after 3 h pre-treatment with the indicated concentration of NAC, PAMAM–$(COOH)_{46}$–$(NAC)_{18}$ conjugate and the corresponding amount of free dendrimer. Three samples were used for each group. The amount of ROS released into the media was measured using Amplex Red. $^{*}P < 0.05$, $^{**}P < 0.01$ vs group of LPS; $^{\blacklozenge}P < 0.05$, $^{\blacklozenge\blacklozenge}P < 0.01$ vs group of NAC in same concentration.

that at 24 h after activation. This is also seen in our studies (Figs. 8 and 9).

3.4.1. ROS assay

ROS has been known to play important roles in oxidation and inflammation. We examined whether PAMAM–$(COOH)_{46}$–$(NAC)_{18}$ conjugate inhibited the release of ROS induced by LPS in BV-2 cells. After 24 h of stimulation with LPS following 3 h pre-treatment, free NAC did not affect ROS production over a concentration range of 0.5–8 mM ($P > 0.05$). In contrast, the PAMAM–$(COOH)_{46}$–$(NAC)_{18}$ conjugate showed significant inhibition of ROS production at 2 mM and 8 mM when compared to the same concentration of free NAC. After 72 h of activation with LPS following 3 h pre-treatment, only the highest concentration of free NAC (8 mM) inhibited ROS release moderately (30%), whereas the lowest concentration of PAMAM–$(COOH)_{46}$–$(NAC)_{18}$ conjugate (0.5 mM) showed inhibition of ROS production (25%). The conjugate significantly inhibited ROS production at 8 mM when compared to the same concentration of free NAC (68%). The inhibition showed a dose-dependent response.

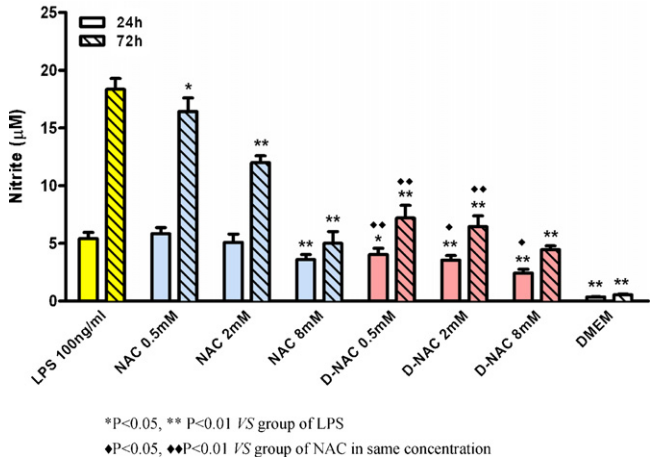

Fig. 9. NO release assay. BV-2 cells (passage 16) were stimulated with 100 ng/mL of LPS for 24 and 72 h after 3 h pre-treatment with the indicated concentration of NAC, PAMAM–$(COOH)_{46}$–$(NAC)_{18}$ conjugate and the corresponding amount of free dendrimer. Three samples were used for each group. Nitrite in culture medium was measured using Griess reagent system. $^{*}P < 0.05$, $^{**}P < 0.01$ vs group of LPS; $^{\blacklozenge}P < 0.05$, $^{\blacklozenge\blacklozenge}P < 0.01$ vs group of NAC in same concentration.

The corresponding concentrations of PAMAM–COOH dendrimer did not affect the cells ROS production after 24 h and 72 h stimulation of LPS following 3 h pre-treatment (Fig. 8, Table 2).

3.4.2. Nitrite assay

After 24 h of activation with LPS following 3 h pre-treatment, only the highest concentration of free NAC (8 mM) significantly reduced nitrite release (~70%), though there was a dose-dependant response. In contrast, the PAMAM–$(COOH)_{46}$–$(NAC)_{18}$ conjugate reduced nitrite release at the lowest equivalent dose of NAC (0.5 mM) (~61%). The conjugate significantly reduced nitrite release at all the three equivalent concentrations compared to free NAC. After 72 h of activation with LPS following 3 h pre-treatment, free NAC reduced nitrite release in a dose-dependent manner. PAMAM–$(COOH)_{46}$–$(NAC)_{18}$ conjugate showed significant reduction of nitrite release even at the lowest concentration (0.5 mM) when compared to the same concentration of free NAC (by ~60%). In fact, 0.5 mM NAC in the conjugated form, showed better efficacy compared to 2 mM of free NAC. The conjugate showed a dose-dependent response (Fig. 9, Table 2). The free PAMAM–COOH dendrimer control slightly decreased the nitrite release only at the highest concentration (0.44 mM) after 72 h stimulation of LPS following 3 h pre-treatment (Fig. 10, Table 2).

3.5. Anti-inflammatory activity of PAMAM–$(COOH)_{46}$–$(NAC)_{18}$ conjugate

Anti-inflammatory activity of PAMAM–$(COOH)_{46}$–$(NAC)_{18}$ conjugate was evaluated *in vitro* using BV-2 cells, which were activated with LPS to induce TNF-α synthesis. In contrast to ROS and NO levels after activation, TNF-α levels have been shown to be appreciably faster, with significant increases at 24 h (Waseem et al., 2008; El-Remessy et al., 2008). This is consistent with the present study, where high TNF-α levels were seen after 24 h. After 24 h and 72 h of activation with LPS following 3 h pre-treatment, *free NAC* inhibited TNF-α production in a dose-dependent manner, with a maximum reduction of ~45% at 8 mM concentration. In comparison, the PAMAM–$(COOH)_{46}$–$(NAC)_{18}$ *conjugate* reduced the TNF-α production very significantly (~67%) even at the lowest equivalent dose of NAC (0.5 mM). Typically, the conjugate showed better efficacy at 0.5 mM compared to free NAC at 8 mM, in all the three assays. The inhibitory effect did not show a significant dose dependence (Fig. 11, Table 2), perhaps because appreciable reduction was seen

Table 2
Inhibitory rate of NAC, conjugate and dendrimer in markers of oxidative stress and inflammation after 72 h stimulation of LPS following 3 h treatment.

	Drug dose	H_2O_2 reduction (%)	Nitrite reduction (%)	TNF-α reduction (%)
NAC	0.5 mM	5.54 ± 6.38	10.52 ± 6.43	34.98 ± 2.43
	2 mM	22.28 ± 8.33	34.66 ± 3.22	35.13 ± 4.44
	8 mM	41.31 ± 2.33	72.70 ± 5.56	44.57 ± 4.35
Dendrimer	0.03 mM	2.09 ± 14.53	−20.16 ± 12.90	−10.21 ± 5.07
	0.11 mM	−9.37 ± 24.63	36.29 ± 17.74	−5.82 ± 4.58
	0.44 mM	−3.16 ± 21.02	46.77 ± 15.32	8.64 ± 6.73
D-NAC	0.5 mM	30.81 ± 8.08	60.82 ± 6.05	67.46 ± 3.91
	2 mM	51.13 ± 4.93	64.85 ± 5.12	74.43 ± 3.54
	8 mM	68.75 ± 4.14	75.75 ± 1.85	77.37 ± 3.31

Inhibitory rate (%) (compared to control) = LPS control group − treatment group/LPS control group × 100%, mean ± SD, $n = 3$.

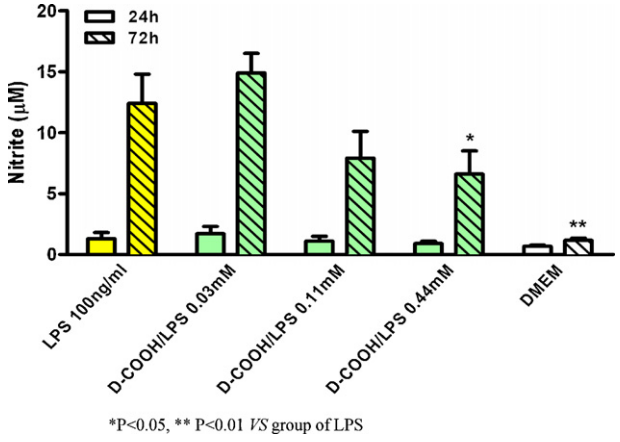

Fig. 10. The effect of dendrimer on NO release. BV-2 cells (passage 16) were stimulated with 100 ng/mL of LPS for 24 h and 72 h after 3 h pre-treatment with the indicated concentration of PAMAM–COOH dendrimer. Three samples were used for each group. Nitrite in culture medium was measured using Griess reagent system. $^{*}P < 0.05$, $^{**}P < 0.01$ vs group of LPS.

even at the lowest dose. The free PAMAM–COOH dendrimer control did not inhibit TNF-α production (Fig. 12, Table 2).

4. Discussion

An anionic dendrimer–NAC conjugate was prepared with a high drug payload. The drug was linked to the dendrimer using a GSH sensitive linker, which released the drug at intracellular GSH concentrations. The cell uptake and the anti-oxidant and anti-inflammatory activity were evaluated in activated microglial cells, which are the target cells for the *in vivo* application in a rabbit model of cerebral palsy.

From the results of flow cytometry and confocal microscopy, it appears that PAMAM–$(COOH)_{62}$–$(FITC)_2$ dendrimer are transported inside the cells efficiently and relatively rapidly. BV-2 cells are known to possess anionic charge, which is the same as that of PAMAM–$(COOH)_{62}$–$(FITC)_2$ dendrimer at physiological pH. Therefore, it may be expected that the cellular entry of PAMAM–$(COOH)_{62}$–$(FITC)_2$ into BV-2 cells may be restricted. Despite this, the cell uptake is significant, perhaps suggesting an active endocytosis mechanism (Kannan et al., 2007; Perumal et al., 2008).

Cytotoxicity assay demonstrated that free NAC, free dendrimer, and the PAMAM–$(COOH)_{46}$–$(NAC)_{18}$ conjugate are relatively non-toxic. Previous work on the cytotoxicty of dendrimers has suggested that the toxicity depends on end functionality, concentration and the time of exposure (Malik et al., 2000). Typically, anionic dendrimers have found to be significantly less toxic than cationic dendrimers. For example, Malik et al. (2000) observed that the PAMAM-G2.5–COOH dendrimer did not exhibit any significant toxicity against B16F10 melanoma cells at 2 mg/mL. The fact that microglial cells do not show measurable cytotoxicity at these levels, allows us to assess the efficacy of the nanodevices at well-defined treatment conditions.

Inflammatory responses in the brain are now thought to be mainly associated with activity of microglial cells, the resident

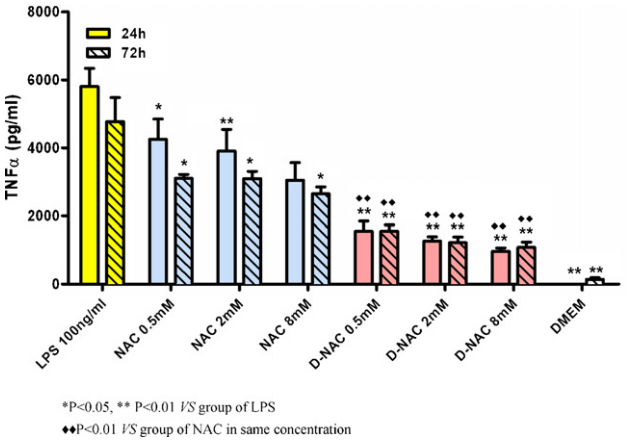

Fig. 11. TNF-α release assay. BV-2 cells (passage 16) were stimulated with 100 ng/mL of LPS for 24 h and 72 h after 3 h pre-treatment with the indicated concentration of NAC and PAMAM–$(COOH)_{46}$–$(NAC)_{18}$ conjugate. Three samples were used for each group. TNF-α in culture medium was measured using mouse TNF-α ELISA Kit. $^{*}P < 0.05$, $^{**}P < 0.01$ vs group of LPS; $^{♦♦}P < 0.01$ vs group of NAC in same concentration.

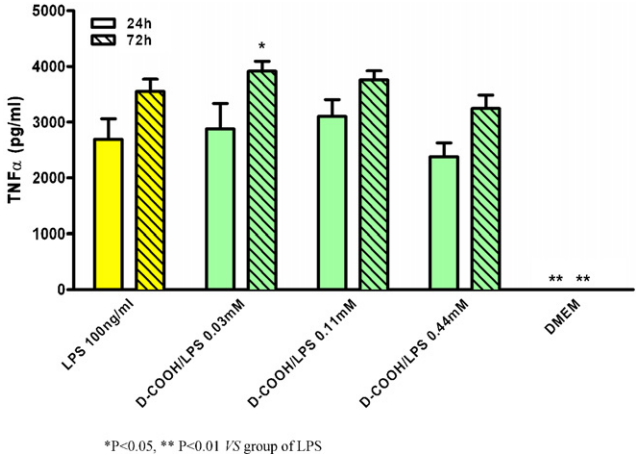

Fig. 12. The effect of dendrimer on TNF-α release. BV-2 cells (passage 16) were stimulated with 100 ng/mL of LPS for 24 h and 72 h after 3 h pre-treatment with the chosen concentration (in mM) of PAMAM–COOH dendrimer. Three samples were used for each group. TNF-α in culture medium was measured using mouse TNF-α ELISA Kit. $^{*}P < 0.05$, $^{**}P < 0.01$ vs group of LPS.

macrophages of CNS, serving the role of immune surveillance and host defense under normal condition. Under pathological conditions, microglial cells become activated and have been implicated as the predominant cell type governing inflammation-mediated neuronal damage. In particular, activated microglial cells exert cytotoxic effects by releasing inflammatory mediators, such as reactive oxygen species (ROS), nitric oxide (NO) and a variety of proinflammatory cytokines such as tumor necrosis factor alpha (TNF-α). In this study, we used LPS to activate BV-2 microglial cells *in vitro*. LPS, the cell wall component of Gram-negative bacterica, is known to activate mitrogen-actived protein kinases, nuclear factor-kB (NF-kB), protein kinase C and tyrosine kinases, which have been implicated in the release of immune-related cytotoxic factors, such as ROS, NO and proinflammatory cytokines (Lu et al., 2007).

In our *in vivo* studies, we seek to use N-acetyl-L-cysteine (NAC) to address neuroinflammation in perinatal brain injury (Makki et al., 2008). Therefore, we evaluated the cellular efficacy of the conjugate in activated BV-2 microglial cells. The anti-oxidative properties of the conjugate were tested by measuring the ROS and NO levels in cell culture medium, and nitrite was chosen as a marker of free radical NO. The anti-inflammatory activity was evaluated by measuring the TNF-α level in cell culture medium. We also compared the efficacy of PAMAM–$(COOH)_{46}$–$(NAC)_{18}$ conjugate on anti-oxidation and anti-inflammation between 24 h or 72 h stimulation of LPS following 3 h pre-treatment.

In our experiment, production of ROS by dysfunctional mitochondria or by xanthine oxidase may contribute to LPS-induced oxidative stress with microglial cells (Paintlia et al., 2007). Peroxisomes are important for detoxification of ROS, and LPS induced effects are known to cause peroxisomal dysfunction which has been linked with ROS generation in apoptosis (Paintlia et al., 2007). NAC can abolish LPS-induced ROS production. The PAMAM–$(COOH)_{46}$–$(NAC)_{18}$ conjugate (8 mM) showed significant therapeutic effect in reducing the ROS release compared to the same concentration of free NAC after 72 h stimulation of LPS following 3 h pre-treatment. Dendrimer did not show any effects on ROS release following short and long time treatment, suggesting that the conjugate is able to transport and release the drug inside the cells.

Nitric oxide (NO) is produced by most cells, and is cytotoxic at high concentration or in the presence of superoxide. The cytotoxic effects are due, at least in part, to the formation of peroxynitrite from NO and superoxide, which represents a strong oxidant and nitrating agent. On that other hand, NO itself can exert cytotoxic effects due to nitrosylation reaction and the inhibition of the mitochondrial respiration by binding to the mitochondrial cytochrome *c* oxidase (Noack et al., 2000). NAC can suppress LPS-induced NO production. The PAMAM–$(COOH)_{46}$–$(NAC)_{18}$ conjugate appears to show better therapeutic effect towards inhibiting activated microglical cells from releasing NO when compared to the same concentration of free NAC after 24 h and 72 h stimulation of LPS following 3 h pre-treatment. We also found that high concentration of free PAMAM–COOH dendrimer significant decrease the concentration of nitrite in medium. The mechanism is perhaps by the binding of the interior secondary amines between dendrimer and nitrite. Therefore, the PAMAM–$(COOH)_{46}$–$(NAC)_{18}$ conjugate may be decreasing the nitrite level in cell culture medium through the effects of *both* NAC and dendrimers.

LPS can also stimulate the secretion of pro-inflammatory cytokines TNF-α, IL-1β and IL-6 in maternal and fetal compartments including fetal brain. Pro-inflammatory cytokines induced severe peroxisomal dysfunction and increased oxidative stress. Anti-inflammatory effects of NAC are attributed to the suppression of pro-inflammatory cytokine expression and release, adhesion molecule expression and activation of NF-κB in cells (Paintlia et al., 2008). The PAMAM–$(COOH)_{46}$–$(NAC)_{18}$ conjugate showed more significant efficacy to inhibit activated microglical cells to release TNF-α when compared to the same concentration of free NAC after 24 h and 72 h stimulation of LPS following 3 h pre-treatment. PAMAM–COOH dendrimer did not reduced TNF-α release.

From these results, it appears that high drug payload in the dendrimer conjugate produces a high local drug concentration inside the cells. The utilization of a GSH sensitive release mechanism is enabling faster drug release and higher pharmacological response compared to the same concentration of free drug. The improved *in vitro* efficacy of the conjugates is a significant result, since most polymer-drug conjugates show less efficacy in cells (partly attributed to slower, inefficient drug release from the conjugates), even though enhanced permeation and retention effect (EPR) and ligand-targeting produces better efficacy *in vivo* (references). Specific to dendrimers, recent studies have shown that the use of an anionic dendrimer and appropriate choice of linking chemistry can produce superior therapeutic efficacies, even in cells, without the use of any targeting moieties (Gurdag et al., 2005; Navath et al., 2008).

The PAMAM–$(COOH)_{46}$–$(NAC)_{18}$ conjugate can be a very good candidate for *in vivo* testing in neuroinflammation models (Makki et al., 2008). By achieving a high local drug concentration with conjugates at the target site one could overcome the systemic adverse effects of free drug and improve the therapeutic efficacy significantly with a reduced dose. Recent studies have shown that the PAMAM dendrimers may have an intrinsic ability to selectively accumulate in cells associated with neuroinflammation, upon local or intravenous delivery (Kannan et al., 2007). When this is combined with the lower cytotoxicity and improved efficacy in the target microglial cells, the potential for superior *in vivo* results could be enhanced. Relative to free drug, this conjugate shows better efficacy compared to ester-linked neutral PAMAM dendrimer–methyl prednisolone conjugate, perhaps due to better intracellular drug release enabled by the disulfide linker (Khandare et al., 2005).

5. Conclusions

A PAMAM–$(COOH)_{46}$–$(NAC)_{18}$ conjugate has been prepared using a disulfide linker, that enables relatively rapid intracellular release of the drug. The FITC-labeled anionic dendrimer is rapidly taken up by microglial cells, despite the anionic surface charge. PAMAM–$(COOH)_{46}$–$(NAC)_{18}$ conjugate is non-toxic even at the higher concentrations tested *in vitro*. PAMAM–$(COOH)_{46}$–$(NAC)_{18}$ conjugate is a more effective anti-oxidant and anti-inflammatory agent when compared to free NAC *in vitro*. The conjugate showed significant efficacy even at the lowest dose (0.5 mM NAC), where the activity was comparable or better than that of Eunice Kennedy Shriver free drug at 8 mM (16× higher dosage). This suggests that dendrimer–NAC conjugates could be effective nanodevices in decreasing inflammation and injury, induced by activated microglial cells in disorders such as cerebral palsy.

Acknowledgment

This study was supported by the Intramural Research Program of the National Institute of Child Health and Human Development, NIH, DHHS, and the Pediatric Critical Care Scientist Development Program NICHD-K08.

References

Alexandre, J., Batteux, F., Nicco, C., Chereau, C., Laurent, A., Guillevin, L., Weill, B., Goldwasser, F., 2006. Accumulation of hydrogen peroxide is an early and crucial step for paclitaxel-induced cancer cell death both *in vitro* and *in vivo*. Int. J. Cancer 119, 41–48.

Cheng, Y., Wang, J., Rao, T., He, X., Xu, T., 2008. Pharmaceutical applications of dendrimers: promising nanocarriers for drug delivery. Front. Biosci. 13, 1447–1471.

El-Remessy, A.B., Tang, Y., Zhu, G., Matragoon, S., Khalifa, Y., Liu, E.K., Liu, J.-Y., Hanson, E., Mian, S., Fatteh, N., Liou, G.I., 2008. Neuroprotective effects of cannabidiol in endotoxin-induced uveitis: critical role of p38 MAPK activation. Mol. Vis. 14, 2190–2203.

Gomez, R., Romero, R., Nien, J., Medine, L., Carstens, M., Kim, Y.M., Espinoza, J., Chaiworapongsa, T., Gonzalez, R., Iams, J.D., Rojas, I., 2007. Antibiotic administration to patients with preterm premature rupture of membranes does not eradicate intra-amniotic infection. J. Matern. Fetal Neonatal Med. 20, 167–173.

Gurdag, S., Khandare, J., Staples, S., Kannan, R.M., Matherly, L., 2005. Activity of dendrimer–methotrexate conjugates in sensitive and resistant cell lines. Bioconjugate Chem. 17, 275–283.

Kannan, S., Kolhe, P., Raykova, V., Glibatec, M., Kannan, R.M., Lai, M.L., Bassett, D., 2004. Dynamics of cellular entry and drug delivery by dendritic polymers into human epithelial carcinoma cells. J. Biomater. Sci. Polym. Edn. 15, 311–330.

Kannan, R.M., Iezzi, R., Rajaguru, B., Kannan, S. Dendrimer-containing particles for sustained release of compounds (US/International patent filed, US Patent application #60/997987).

Khandare, J., Kolhe, P., Pillai, O., Kannan, S., Lai, M.L., Kannan, R.M., 2005. Synthesis, cellular transport, and activity of polyamidoamine dendrimer–methylprednisolone conjugates. Bioconjugate Chem. 16, 330–337.

Kim, M.Y., Wogan, G.N., 2006. Mutagenesis of the supF gene of pSP189 replicating in AD293 cells cocultivated with activated macrophages: roles of nitric oxide and reactive oxygen species. Chem. Res. Toxicol. 19, 1483–1491.

Kolhe, P., Khandare, J., Pillai, O., Kannan, S., Lai, M.L., Kannan, R.M., 2006. Preparation cellular transport, and activity of polyamidoamine-based dendritic nanodevices with a high drug payload. Biomaterials 17, 660–669.

Kolhe, P., Misra, E., Kannan, R.M., Kannan, S., Lai, M.-L., 2003. Drug complexation, in vitro release and cellular entry of dendrimers and hyperbranched polymers. Int. J. Pharm. 259, 143–160.

Kurtoglu, Y.E., Navath, R., Wang, B., Kannan, S., Romero, R., Kannan, R.M., 2009. Poly(amidoamine) dendrimer–drug conjugates with disulfide linkages for intracellular drug delivery. Biomaterials 30, 2112–2121.

Lee, C.C., MacKay, J.A., Fréchet, J.M.J., Szoka, F.C., 2005. Designing dendrimers for biological applications. Biotechnology 23, 1517–1526.

Lessio, C., Assunc, F.D., Gloria, A.M., Beatriz, A., Tommaso, G.D., Mouro, M.G., Marco, G.S.D., Schor, N., Higa, E.M.S., 2005. Cyclosporine A and NAC on the inducible nitric oxide synthase expression and nitric oxide synthesis in rat renal artery cultured cells. Kidney Int. 68, 2508–2516.

Lu, D.Y., Tang, C.H., Liou, H.C., Teng, C.M., Jeng, K.C.G., Kuo, S.C., Lee, F.Y., Fu, W.M., 2007. YC-1 attenuates LPS-induced proinflammatory responses and activation of nuclear factor-kB in microglia. Br. J. Pharmacol. 151, 396–405.

Makki, F.S., Kannan, S., Lu, Janisse, X., Dawe, J.E., Edwin, S., Romero, R., Chugani, D., 2008. Intrauterine administration of endotoxin leads to motor deficits in a rabbit model: a link between prenatal infection and cerebral palsy. Am. J. Obstet. Gynecol. 199, 651–1651.

Malik, N., Wiwattanapatapee, R., Klopsch, R., Lorenz, K., Frey, H., Weener, J.W., Meijer, E.W., Paulus, W., Duncan, R., 2000. Dendrimers relationship between structure and biocompatibility in vitro, and preliminary studies on the biodistribution of 125I-labelled polyamidoamine dendrimers in vivo. J. Control. Release 65, 133–148.

Min, K.J., Jou, I., Joe, E., 2003. Plasminogen-induced IL-1B and TNFa production in microglia is regulated by reactive oxygen species. Biochem. Biophys. Res. Commun. 312, 969–974.

Navath, R.S., Kurtoglu, Y.E., Wang, B., Kannan, S., Romero, R., Kannan, R.M., 2008. Dendrimer–drug conjugates for tailored intracellular drug release based on glutathione levels. Bioconjugate Chem. 19, 2446–2455.

Noack, H., Possel, H., Chatterjee, S., Keilhoff, G., Wolf, G., 2000. Nitrosative stress in primary glial cultures after induction of the inducible isoform of nitric oxide synthase (i-NOS). Toxicology 148, 133–142.

Paintlia, M.K., Paintlia, A.S., Contreras, M.A., Singh, I., Singh, A.K., 2008. Lipopolysaccharide-induced peroxisomal dysfunction exacerbates cerebral white matter injury: attenuation by N-acetyl cysteine. Exp. Neurol. 210, 560–576.

Perumal, O., Rajyalakshmi, I., Kannan, S., Kannan, R.M., 2008. The effect of surface functionality on cellular trafficking of dendrimers. Biomaterials 29, 3469–3476.

Romero, R., Gomez, R., Ghezzi, F., Yoon, B.H., Mazor, M., Edwin, S., Berry, S., 1998. A fetal systemic inflammatory response is followed by the spontaneous onset of preterm parturition. Am. J. Obstet. Gynecol. 179, 186–193.

Romero, R., Gotsch, F., Pineles, B., Kusanovic, J.P., 2007a. Inflammation in pregnancy: its roles in reproductive physiology, obstetrical complications, and fetal injury. Nutr. Rev. 65, S194–S202.

Romero, R., Espinoza, J., Goncalves, L.F., Kusanovic, J.P., Friel, L., Hassan, S., 2007b. The role of inflammation and infection in preterm birth. Semin. Reprod. Med. 25, 21–39.

Romero, R., Espinoza, J., Kusanovic, J.P., Gotsch, F., Hassan, S., Erez, O., Chaiworapongs, T., Mazorc, M., 2006. The preterm parturition syndrome. Int. J. Obstet. Gynaecol. 113, 17–42.

Roy, A., Jana, A., Yatish, K., Freidt, M.B., Fung, Y.K., Martinson, J.A., Pahan, K., 2008. Reactive oxygen species up-regulate CD11b in microglia via nitric oxide: implications for neurodegenerative diseases. Free Radic. Biol. Med. 26, 116–121.

Villalonga-Barber, C., Micha-Screttas, M., Steele, B.R., 2008. Dendrimers as biopharmaceuticals: synthesis and properties. Curr. Top. Med. Chem. 8 (14), 1294–1309.

Wang, X., Svedin, P., Nie, C., Lapatto, R., Zhu, C., Gustavsson, M., Sandberg, M., Karlsson, J.O., Romero, R., Hagberg, H., Mallard, C., 2007. N-acetylcysteine reduces lipopolysaccharide-sensitized hypoxic–ischemic brain injury. Ann. Neurol. 61, 263–271.

Waseem, T., Duxbury, M., Ito, H., Ashley, S.W., Robinson, M.K., 2008. Exogenous ghrelin modulates release of pro-inflammatory and anti-inflammatory cytokines in LPS stimulated macrophages through distinct signaling pathways. Surgery 143, 334–342.

Wiwattanapatapee, R., Gómez, B.C., Malik, N., Duncan, R., 2004. Anionic PAMAM dendrimers rapidly cross adult rat intestine in vitro: a potential oral delivery system. Pharm. Res. 2, 991–998.

Wolinsky, J.B., Grinstaff, M.W., 2008. Therapeutic and diagnostic applications of dendrimers for cancer treatment. Adv. Drug Deliv. Rev. 60 (9), 1037–1055.